An approximate model for estimating the faradaic efficiency loss in zinc/bromine batteries caused by cell self-discharge

Shian-Cherng Yang

Industrial Technology Research Institute, Energy and Resources Laboratories, Chutung, Hsinchu, Taiwan 310 (Taiwan)

(Received April 2, 1993; in revised form January 17, 1994; accepted January 21, 1994)

Abstract

An approximate mathematical model for estimating the faradaic efficiency loss in zinc/bromine batteries caused by the cell self-discharge is described. Parametric studies have been performed to determine the effects on the cell self-discharge of the volume of oil phase in the electrolyte storage tank, the bromine distribution coefficient of the quaternary ammonium salts, the equivalent thickness of the microporous plastic separator, and the hydrodynamic flow condition in the electrolyte chambers. A discussion is presented based on these parametric investigations.

Introduction

The zinc/bromine (Zn/Br_2) system with circulating electrolyte is a promising advanced secondary battery for energy storage. Inherent attractive features include the use of relatively low-cost materials, high energy density, simple electrode kinetics, an aqueous electrolyte system, and operation at room temperature. Furthermore, because of the use of conductive carbon plastic as the electrode material, the battery is very suitable for mass production and assembly at low cost [1]. To date, the battery system has been developed to quite a large scale, and tested in electric vehicle and load levelling applications [2, 3].

A major problem with Zn/Br_2 batteries is the cell self-discharge. This is caused by the transport of bromine and tribromide ion from the bromine electrode to the zinc electrode [1, 4, 5]. If the cell is to be operated at an acceptable faradaic efficiency, the rate of this transport process must be restricted to a low level. A common approach to controlling this rate is to incorporate quaternary ammonium salts in the aqueous electrolyte. During battery charging, the major part of the generated bromine will then be in the form of oil phase through complexing with the quaternary ammonium salts and, thereby, a low concentration of bromine and tribromide ion will be maintained in the aqueous electrolyte. During cell operation, the main factors that influence the cell self-discharge may include: the electrolyte formulation; the hydrodynamic flow condition of the electrolytes, the quaternary ammonium salts, and the properties of the separator.

In this paper, an approximate model for estimating the faradaic efficiency loss in Zn/Br_2 batteries caused by cell self-discharge is described. Parametric studies with

SSDI 0378-7753(94)01910-N

the model serve to elucidate the effects on the cell self-discharge of the volume of oil phase in the electrolyte storage tank, the bromine distribution coefficient of the quaternary ammonium salts, the equivalent thickness of the microporous plastic separator, and the hydrodynamic flow condition in the electrolyte chambers. A discussion is presented based on these parametric studies.

Mathematical model

Assumptions

A schematic of a single Zn/Br_2 cell is presented in Fig. 1. The following assumptions are made in the development of the model for describing the cell self-discharge.

(i) For each electrode in the cell, the concentrations of the reactive species leaving the electrode are the inlet values for the electrolyte storage tank on that electrode side. Meanwhile, the concentrations of the reacting species leaving the electrolyte storage tank on each electrode side are the inlet values for that electrode in the cell.

(ii) A homogeneous complexation reaction occurs in the aqueous solution bulk, i.e.:

$$Br_2 + Br^- \rightleftharpoons Br_3^- \tag{1}$$

It is assumed that this reaction is both fast and in equilibrium, according to the equilibrium constant [6]:

$$K_{eq} = \frac{C_{Br_3^-}}{C_{Br^-} C_{Br_2}} = 17 M^- \tag{2}$$

(Note the definitions of the parameters in eqn. (2), and subsequent eqns., are given in the List of symbols at the end of this paper.)

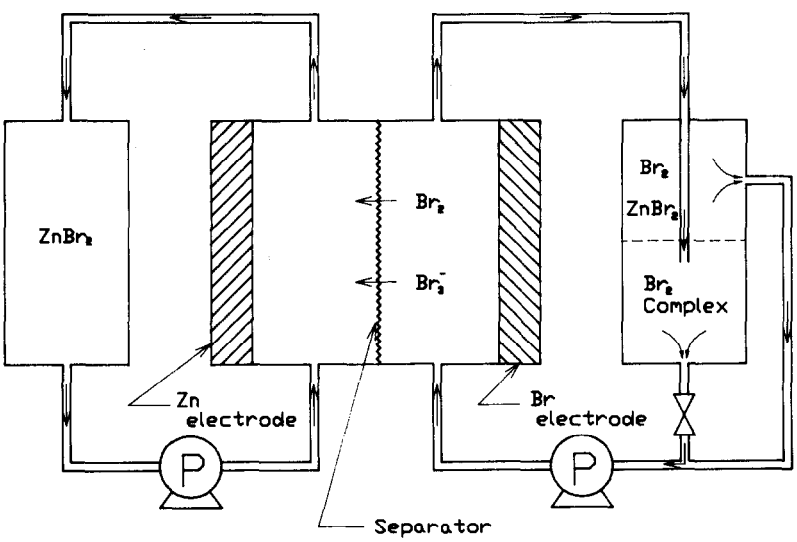

Fig. 1. Simplified diagram of Zn/Br_2 battery system.

(iii) The aqueous and oil phases of the electrolyte for the bromine electrode are at equilibrium. The partition of bromine in these two phases can be expressed by the distribution coefficient, D [7]:

$$D = \frac{C_{Br_2,\,oil}}{C_{Br_2} + C_{Br_3^-}} \tag{3}$$

The distribution coefficient may be affected by the electrolyte composition in the aqueous phase. In this paper, the distribution coefficient is assumed to be constant during the cell operation.

(iv) The volume of the oil phase may be affected by the bromine content that it contains. The oil phase volume is assumed to be approximately constant throughout the cell operation.

(v) The solubilities of bromide and tribromide ions in the oil phase of the electrolyte are negligible.

(vi) As the conversion per pass of the bromine electrode during its operation is very low, a finite difference expression over the length of the electrode can be used to replace the axial concentration gradient. Moreover, the concentration of bromine and tribromide ions in the zinc electrode electrolyte can also be neglected due to the rapid reaction of them on the zinc electrode surface [7]. Under this condition, the average transport flux of bromine and tribromide ions through the separator can be approximately expressed as:

$$N_{Br_2} = 0.5K_{Br_2,\,ov}(C_{Br_2} + C^{out}_{Br_2}) \tag{4}$$

$$N_{Br_3^-} = 0.5K_{Br_3^-,\,ov}(C_{Br_3^-} + C^{out}_{Br_3^-}) \tag{5}$$

(vii) For reducing the complexity in handling the mass balance of the bromide ion in the bromine electrode electrolyte, the effect of zinc complexing with bromide ion on the equilibrium concentration of the bromide ion in the aqueous phase was not considered in this work.

(viii) During cell operation, because of the low concentrations of Br_3^- and Br_2, the transport of these species across the separator from the cell chamber on the bromine electrode side can be reasonably assumed to be achieved mainly by diffusion. Since the bromide ion has a relatively high concentration in both the anolyte and catholyte, it can be assumed that its transport through the separator is determined mainly by migration; the average transport flux can be expressed by:

$$N_{Br^-} = \frac{t_{Br^-} i}{f} \tag{6}$$

(ix) During cell operation, it is assumed that there is no accumulation of bromine, tribromide ion or bromide ion in the bromine electrode in the cell.

(x) Only the cell self-discharge caused by the transport of bromine and tribromide ion in the aqueous phase of the electrolyte through the separator is considered in calculating the cell faradaic efficiency.

Model development

Mass transport through separator

The electrolyte flowing into the bromide electrode is a two-phase flow that comprises an aqueous and a polybromide oil phase (the oil phase is in dispersed state). The bromine in the electrolyte is distributed between both the phases, but the tribromide ion is present only in the aqueous phase. During cell operation, the bromine

and tribromide ion will be transported through the separator from the electrolyte chamber on the bromine electrode side to that on the zinc electrode side. The overall mass-transfer coefficient and the mass flux for this transport is given by [8]:

$$\frac{1}{K_{i,\,ov}} = \frac{1}{K_{i,\,C}} + \frac{1}{P_{i,\,S}} + \frac{1}{K_{i,\,A}} \tag{7}$$

$$N_i = K_{i,\,ov}(C_i - C_{i,\,A}) \tag{8}$$

where $P_{i,\,S}$ is the permeability coefficient for the species i diffusing through the separator and expressed as:

$$P_{i,\,S} = \frac{D_i}{d_S} \tag{9}$$

where d_S is the equivalent thickness of the separator. The latter parameter may be regarded as the thickness of stagnant electrolyte that will allow the same rate of species transport as does the separator [9]. The parameters $K_{i,\,C}$ and $K_{i,\,A}$ are the mass-transport coefficients of species i on the bromine and zinc electrode sides of the separator, respectively. For electrolyte in the electrolyte chamber in a laminar flow region, the Reynolds number is:

$$Re = \frac{d_h \nu}{\nu} \tag{10}$$

where the hydraulic diameter, d_h, is used as the characteristic length and given as:

$$d_h = \frac{4bh}{2(b+h)} \tag{11}$$

For single-phase flow, Roušar *et al.* [10] presented the following correlation for determining the convective mass-transfer coefficient for undeveloped laminar mass transport in channels:

$$Sh_{av} = 1.85\chi\left(ReSc\,\frac{d_h}{l}\right)^{1/3} \tag{12}$$

where χ is a correction factor that considers the geometry of the flow channel; the dimensionless groups of Sh_{av} and Sc are:

$$Sh_{av} = Kd_h/D_i \tag{13}$$

$$Sc = \frac{\nu}{D_i} \tag{14}$$

For two-phase flow, Lu and Alkire [11] propose that the overall mass-transfer rate can be separated into three elements: (i) a single-phase mass-transfer rate; (ii) an enhancement of the mass-transfer rate due to the disturbance mechanism, and (3) an enhancement of the mass-transfer rate due to the extraction mechanism. Therefore, the overall mass-transfer coefficient for a two-phase flow is modelled as [11]:

$$K = k_1 + k_2 + k_3\,\frac{C_2}{C_1} \tag{15}$$

where k_1 is the mass-transfer coefficient due to one-phase flow, k_2 the mass-transfer coefficient due to the disturbance mechanism, k_3 the mass-transfer coefficient due to

the extraction mechanism, C_2 is the reactant concentration in the second phase (dispersed phase), and C_1 is the reactant concentration in the continuous phase. The factors that influence k_2 and k_3 are quite complicated and include: the dispersed phase volume fraction, droplet size, flow velocity, and presence of a turbulence promoter [11].

The tribromide ion resides only in the aqueous phase of the electrolyte. Thus, $K_{Br_3^-,C}$ can be calculated according to eqn. (12). For $K_{Br_2,C}$, the mass-transport coefficient on the bromine electrode side can be calculated according to eqn. (15), due to its distribution in both the aqueous and the oil phases of the electrolyte.

Because it has been assumed that there is both a negligible concentration of bromine and tribromide ions in the electrolyte chamber on the zinc electrode side and a low conversion of the reacting species per pass during the cell operation, the following two equations can be obtained. Furthermore, the average mass flux of the bromine and tribromide ions being transported from the electrolyte chamber on the bromine electrode side to that on the zinc electrode side can be determined according to eqns. (4) and (5), i.e.:

$$C_{i,A}=0 \tag{16}$$

$$C_i^{av}=0.5(C_i+C_i^{out}) \tag{17}$$

where the subscript 'A' represents the anode (zinc electrode).

Material balance

For the cell, the electrochemical reaction taking place on the bromine electrode is:

$$0.5Br_2+e^- \rightleftharpoons Br^- \tag{18}$$

and the reacting species of the bromine electrode are bromine and bromide ion. The bromine is partitioned in both the aqueous and the oil phases of the electrolyte. The bromine in the aqueous phase can be in the form of free Br_2 and Br_3^- by complexing with the bromide ion, and the bromine in the oil phase is in the form of a polybromide by complexing with the quaternary ammonium salts. The bromide ion is distributed in the aqueous phase of the electrolyte, and it can be in the form of free Br^- and Br_3^- by complexing with Br_2. The material balance relations for the reacting species of the Br_2 and Br^- added in the electrolyte storage tank of the bromine electrode can be represented by eqns. (19) and (20), respectively:

$$\frac{d}{dt}(C_{Br_2,oil}V_{oil}+C_{Br_2}V_{aq}+C_{Br_3^-}V_{aq})=F_{aq}(C_{Br_2}^{out}+C_{Br_3^-}^{out})+F_{oil}C_{Br_2,oil}^{out}$$

$$-F_{aq}(C_{Br_2}+C_{Br_3^-})-F_{oil}C_{Br_2,oil} \tag{19}$$

$$\frac{d}{dt}(C_{Br^-}V_{aq}+C_{Br_3^-}V_{aq})=F_{aq}(C_{Br^-}^{out}+C_{Br_3^-}^{out}-C_{Br^-}-C_{Br_3^-}) \tag{20}$$

Based on the Faraday's law, the material balance relations for the Br_2 and Br^- in the bromine electrode in the cell are given as follows:

$$F_{aq}(C_{Br_2}^{out}+C_{Br_3^-}^{out}-C_{Br_2}-C_{Br_3^-})+F_{oil}(C_{Br_2,oil}^{out}-C_{Br_2,oil})$$

$$=\frac{-iA}{n_1f}-(N_{Br_2}+N_{Br_3^-})A \tag{21}$$

$$F_{aq}(C_{Br^-}^{out}+C_{Br_3^-}^{out}-C_{Br^-}-C_{Br_3^-})=\frac{iA}{n_2f}-(N_{Br^-}+N_{Br_3^-})A \tag{22}$$

where i is the cell operating current density, and $n_1=2$ and $n_2=1$, according to eqn. (18). The current density i is positive as the cell is discharging, and negative as the cell is charging.

By substituting eqn. (21) in eqn. (19), the material balance relation for the bromine in the electrolyte storage tank becomes:

$$\frac{d}{dt}(C_{Br_2,\,oil}V_{oil}+C_{Br_2}V_{aq}+C_{Br_3^-}V_{aq})=\frac{-iA}{n_1f}-(N_{Br_2}+N_{Br_3^-})A \tag{23}$$

The material balance relation for the bromide ion in the electrolyte storage tank can also be obtained from eqns. (20) and (22) and becomes:

$$\frac{d}{dt}(C_{Br^-}V_{aq}+C_{Br_3^-}V_{aq})=\frac{iA}{n_2f}-(N_{Br^-}+N_{Br_3^-})A \tag{24}$$

From eqns. (2) and (3), the $C_{Br_2,\,oil}$ and $C_{Br_3^-}$ can be expressed as:

$$C_{Br_3^-}=K_{eq}C_{Br^-}C_{Br_2} \tag{25}$$

$$C_{Br_2,\,oil}=D(C_{Br_2}+K_{eq}C_{Br^-}C_{Br_2}) \tag{26}$$

By substituting eqns. (25) and (26) in eqns. (23) and (24), the following two equations can be obtained:

$$(DV_{oil}+DV_{oil}K_{eq}C_{Br^-}+V_{aq}+V_{aq}K_{eq}C_{Br^-})\frac{dC_{Br_2}}{dt}$$
$$+(DV_{oil}K_{eq}C_{Br_2}+V_{aq}K_{eq}C_{Br_2})\frac{dC_{Br^-}}{dt}$$
$$=\frac{-iA}{n_1f}-(N_{Br_2}+N_{Br_3^-})A \tag{27}$$

$$C_{Br^-}V_{aq}K_{eq}\frac{dC_{Br_2}}{dt}+V_{aq}(1+K_{eq}C_{Br_2})\frac{dC_{Br^-}}{dt}$$
$$=\frac{iA}{n_2f}-(N_{Br^-}+N_{Br_3^-})A \tag{28}$$

The solutions of dC_{Br_2}/dt and dC_{Br^-}/dt in the above two simultaneous equations are:

$$\frac{dC_{Br_2}}{dt}=\frac{C_1B_2-C_2B_1}{A_1B_2-A_2B_1} \tag{29}$$

$$\frac{dC_{Br^-}}{dt}=\frac{A_1C_2-A_2C_1}{A_1B_2-A_2B_1} \tag{30}$$

where A_1, B_1, C_1, A_2, B_2, and C_2 are defined as follows:

$$A_1=DV_{oil}+DV_{oil}K_{eq}C_{Br^-}+V_{aq}+V_{aq}K_{eq}C_{Br^-} \tag{31}$$

$$B_1=DV_{oil}K_{eq}C_{Br_2}+V_{aq}K_{eq}C_{Br_2} \tag{32}$$

$$C_1=\frac{-iA}{n_1f}-(N_{Br_2}+N_{Br_3^-})A \tag{33}$$

$$A_2 = C_{Br^-} V_{aq} K_{eq} \tag{34}$$

$$B_2 = V_{aq}(1 + K_{eq} C_{Br_2}) \tag{35}$$

$$C_2 = \frac{iA}{n_2 f} - (N_{Br^-} + N_{Br_3^-})A \tag{36}$$

In order to calculate N_{Br_2} and $N_{Br_3^-}$ in eqns. (33) and (36), $C_{Br_2}^{out}$ and $C_{Br_3^-}^{out}$ must be known. They can be determined by solving the following two equations, which are obtained by substituting the $C_{Br_2,\,oil}$ and $C_{Br_3^-}$ in eqns. (25) and (26) in eqns. (21) and (22):

$$F_{aq}(C_{Br_2}^{out} + K_{eq} C_{Br^-}^{out} C_{Br_2}^{out}) + F_{oil} D(C_{Br_2}^{out} + K_{eq} C_{Br^-}^{out} C_{Br_2}^{out})$$

$$= \frac{-iA}{n_1 f} + F_{aq}(C_{Br_2} + C_{Br_3^-}) + F_{oil} C_{Br_2,\,oil} - (N_{Br_2} + N_{Br_3^-})A \tag{37}$$

$$F_{aq}(C_{Br^-}^{out} + K_{eq} C_{Br^-}^{out} C_{Br_2}^{out}) = \frac{iA}{n_2 F} + (C_{Br^-} + C_{Br_3^-})F_{aq} - (N_{Br^-} + N_{Br_3^-})A \tag{38}$$

The initial conditions for C_{Br_2} and C_{Br^-} in the differential equations of eqns. (29) and (30) can be obtained by solving:

$$n_{Br_2}^0 = V_{aq}(C_{Br_2}^0 + C_{Br_3^-}^0) + V_{oil} C_{Br_2,\,oil}^0 \tag{39}$$

$$n_{Br^-}^0 = V_{aq}(C_{Br^-}^0 + C_{Br_3^-}^0) \tag{40}$$

where $C_{Br_3^-}^0$ and $C_{Br_2,\,oil}^0$ can be expressed in the terms of $C_{Br_2}^0$ and $C_{Br^-}^0$ by using eqns. (25) and (26).

The mole fraction of Br_2 in the oil phase of the electrolyte in the electrolyte storage tanks is given by:

$$X_{Br_2,\,oil} = \frac{C_{Br_2,\,oil} V_{oil}}{(C_{Br_2} + C_{Br_3^-})V_{aq} + C_{Br_2,\,oil} V_{oil}} \tag{41}$$

and the voltage drop across the separator is calculated according to:

$$\Delta V_S = \frac{|i| d_S}{\kappa_S} \tag{42}$$

Numerical techniques were employed to solve the differential equations and the simultaneous algebra equations. The Runge–Kutta method was used to solve eqns. (29) and (30), and the Newton–Raphson method was used to solve eqns. (37) and (38), and (39) and (40).

Faradaic efficiency

Because only faradaic efficiency loss caused by the transport of Br_2 and Br_3^- through the separator is considered in this work, the cell faradaic efficiency at any instant of time can be calculated according to:

$$\epsilon_i = \frac{|i| - 2f(N_{Br_2} + N_{Br_3^-})}{|i|} \tag{43}$$

The average faradaic efficiency for the cell operating over a certain time period is given by:

$$\epsilon_i^{av} = \frac{\int_0^T \epsilon_i \, dt}{T} \tag{44}$$

Results and discussion

A series of simulations have been run for situations in which the cell is being discharged. The purpose of these simulations is to explore the effects on the cell self-discharge of the volume of oil phase in the electrolyte storage tank, the bromine distribution coefficient of the quaternary ammonium salts, the equivalent thickness of the microporous plastic separator, and the hydrodynamic flow condition in the electrolyte chambers. The values of the model parameters used with fixed values in all simulations are given in Table 1.

Eleven simulation cases with different values of the volume of the oil phase in the electrolyte storage tank, the bromine distribution coefficient, the separator equivalent

TABLE 1

Important assumed model parameters

Operating condition	
Cell discharging time	240 min
Volume of aqueous phase in the electrolyte storage tank	100 cm^3
Volume of oil phase in the electrolyte storage tank	50 cm^3
Volume flow velocity of the aqueous phase into the cell chamber	13.5 $cm^3\ s^{-1}$
Volume flow velocity of the oil phase into the cell chamber	1.5 $cm^3\ s^{-1}$
Moles of initially added Br_2	0.12 mol
Moles of initially added Br^-	0.4 mol
Transference number of Br^-	0.15
Discharge current density	0.01 A cm^{-2}
Electrolyte conductivity	0.182 $\Omega^{-1}\ cm^{-1}$
Cell dimension	
Electrode length	10 cm
Width of electrolyte chamber	10 cm
Thickness of electrolyte chamber	0.2 cm
Parameters for the bromine electrode	
Electrolyte kinematic viscosity	$1.3\times10^{-2}\ cm^2\ s^{-1}$
Electrolyte flow velocity in electrolyte chamber	7.5 $cm\ s^{-1}$
Diffusivity of Br_2 in the electrolyte	$7.28\times10^{-6}\ cm^2\ s^{-1}$
Diffusivity of Br_3^- in the electrolyte	$7.28\times10^{-6}\ cm^2\ s^{-1}$
Separator equivalent thickness	0.05 cm
Parameters for the zinc electrode	
Electrolyte kinematic viscosity	$1.1\times10^{-2}\ cm^2\ s^{-1}$
Electrolyte flow velocity in electrolyte chamber	1 $cm\ s^{-1}$
Diffusivity of Br_2 in the electrolyte	$1.06\times10^{-5}\ cm^2\ s^{-1}$
Diffusivity of Br_3^- in the electrolyte	$1.06\times10^{-5}\ cm^2\ s^{-1}$

TABLE 2

Nine cases used for simulating cell self-discharge

	Case no.								
	1	2	3	4	5	6	7	8	9
V_{oil} (ml)	50	25	75	100	50	50	50	50	50
D	20	20	20	20	30	40	20	20	20
d_S (cm)	0.05	0.05	0.05	0.05	0.05	0.05	0.04	0.076	0.2

TABLE 3

Four cases used for studying the effect of electrolyte volume flow velocity on cell self-discharge

	Case no.			
	1	10	9	11
d_S (cm)	0.05	0.05	0.2	0.2
F_{aq} (ml sec^{-1})	13.5	67.5	13.5	67.5
F_{oil} (ml sec^{-1})	1.5	7.5	1.5	7.5
F_{Zn} (ml sec^{-1})	2	10	2	10

thickness, and the electrolyte flow velocity are studied. Tables 2 and 3 give the input values for these parameters. For all the simulation cases, the volume fraction of the oil phase in the inlet electrolyte to the bromine electrode is fixed at 0.1, and the k_2 and k_3 values in eqn. (15) are set equal to k_1 and $0.1k_1$, respectively, according to ref. 11. The simulation results indicate that the conversion per pass for the bromine electrode is never greater than 0.7%.

Volume of oil phase in electrolyte storage tank

The electrolyte for the bromine electrode contains mainly $ZnBr_2$, Br_2, quaternary ammonium salt, and a supporting electrolyte such as KCl or NH_4Cl. For a given amount of the reacting species of bromine and bromide ion, the amount of water and quaternary ammonium salt added to prepare the electrolyte will determine the equilibrium concentration of bromine and tribromide ions in the aqueous phase of the electrolyte in the electrolyte storage tank.

In this work, the amount of bromide ion, bromine, and water initially added to prepare the electrolyte for the bromine electrode was fixed. By varying the volume of the oil phase in the electrolyte storage tank, its effect on the cell self-discharge was studied. The resulting cell faradaic efficiency and the C_{Br_2}, $C_{Br_3^-}$, C_{Br^-}, and $C_{Br_2,\,oil}$ during the cell operating period are given in Figs. 2 to 6. Also, the average cell faradaic efficiency over the operating period and the initial mole fraction of Br_2 in the oil phase in the electrolyte storage tank are listed in Table 4.

The data indicate several important trends.

(i) The concentrations of Br_2 and Br_3^- in the aqueous phase of the electrolyte decrease with increase in the volume of the oil phase in the electrolyte storage tank.

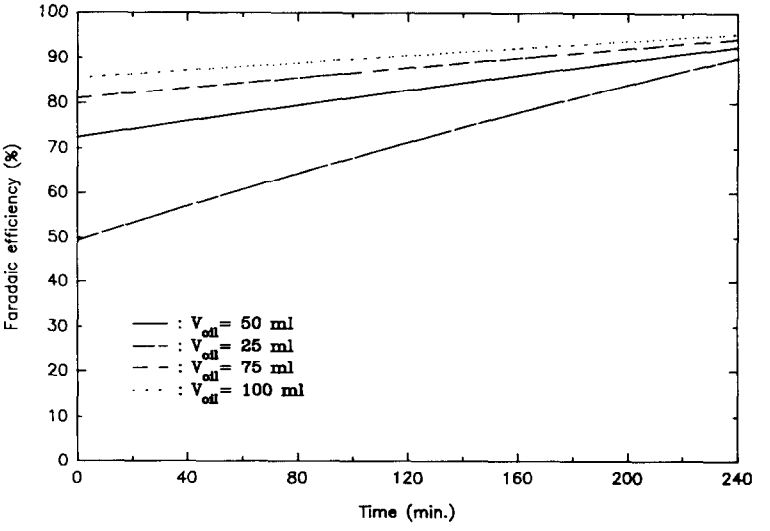

Fig. 2. Faradaic efficiency over cell discharge period for cases with different oil phase volumes.

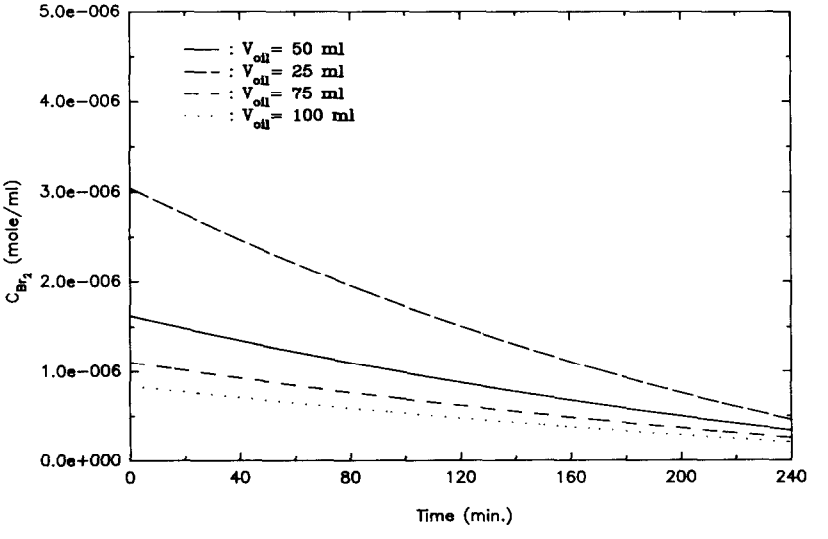

Fig. 3. Concentration of bromine in aqueous phase of the electrolyte over cell discharge period for cases with different oil phase volumes.

Figures 3 and 4 demonstrate that the concentration variation in these two species caused by the difference in the oil phase volume will become less significant, compared with the increase in the volume of the oil phase.

(ii) The major portion of the Br_2 in the aqueous phase of the electrolyte is in the form of tribromide ions. This is to be expected because of the large amount of bromide ions supplied from the $ZnBr_2$ used.

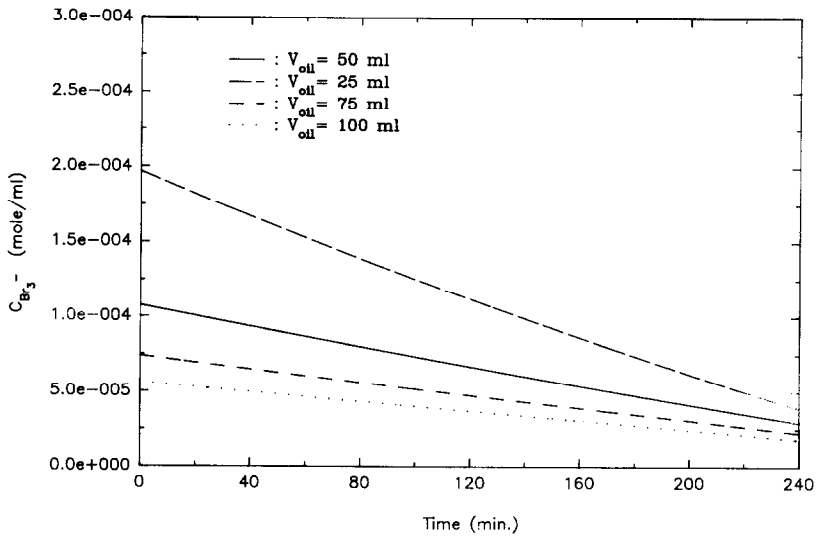

Fig. 4. Concentration of tribromide ions in aqueous phase of the electrolyte over cell discharge period for cases with different oil phase volumes.

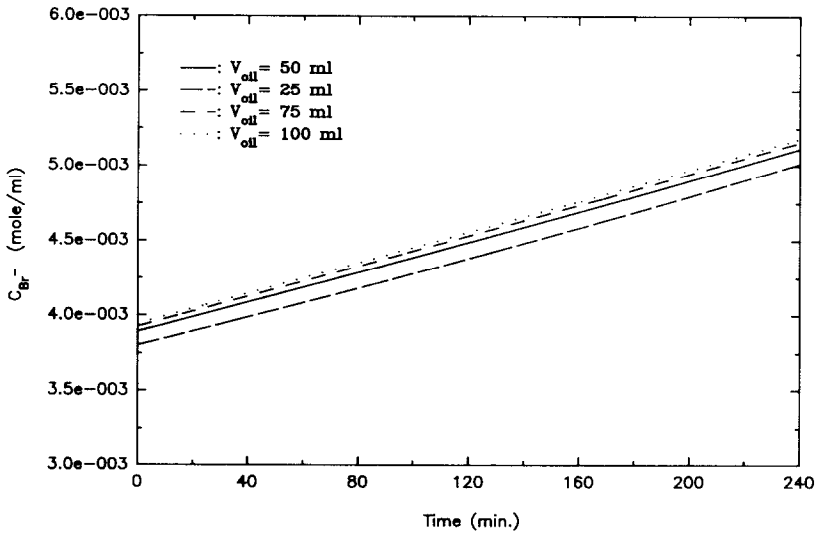

Fig. 5. Concentration of bromide ions in aqueous phase of the electrolyte over cell discharge period for cases with different oil phase volumes.

(iii) The variation in the concentration of the bromide ions in the aqueous phase caused by the difference in the oil phase volume is not significant. The reason for this is that the amount of the bromide ion in the electrolyte added initially is much larger than that of the bromine, and the oil phase volume of the electrolyte can only exert an effect on the bromine partition in the aqueous and oil phases.

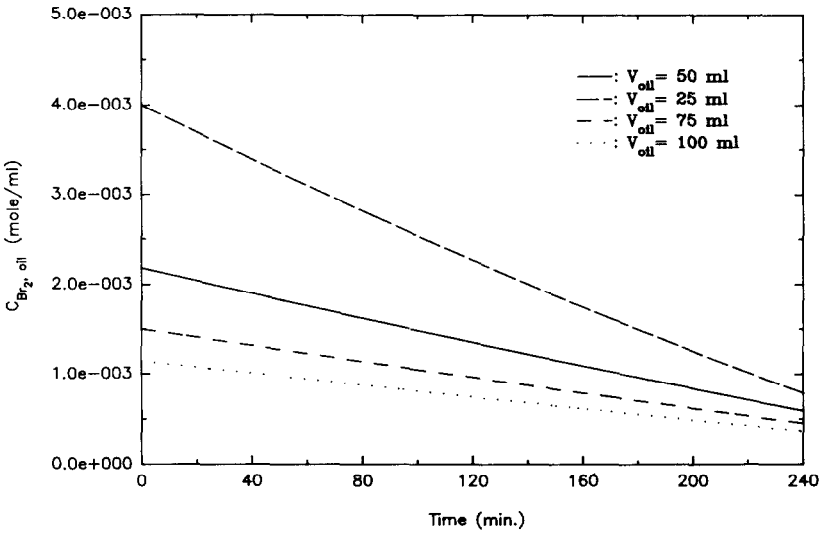

Fig. 6. Concentration of bromine in the oil phase of the electrolyte over cell discharge period for cases with different oil phase volumes.

TABLE 4

Average cell faradaic efficiency and initial mole fraction of Br_2 in the oil phase in the electrolyte storage tank for four selected cases with different V_{oil} values

	Case no.			
	1	2	3	4
ϵ_i^{av} (%)	82.76	70.78	87.80	90.55
$X^0_{Br2, oil}$	0.909	0.833	0.938	0.952

(iv) Figure 2 shows that, for a given quaternary ammonium salt, the improvement in the cell faradaic efficiency by increasing the oil phase volume becomes small when the oil phase volume is beyond a certain value.

(v) Considering both the cell energy density and average faradaic efficiency, Fig. 2 indicates that the use of a larger volume of the oil phase will raise the cell faradaic efficiency. It will, however, also contribute to a decrease in the cell energy density due to the weight increase from the oil phase. Thus, there should exist an optimal volume for the oil phase.

Bromine distribution coefficient of quaternary ammonium salts

In choosing the quaternary ammonium salts for use in the cell, it is necessary to consider first the effect on the partition of bromine between the aqueous and oil phases of the electrolyte. For salts with large bromine distribution coefficients, a larger portion of the bromine will be partitioned in the oil phase of the electrolyte. Nevertheless, other aspects may be equally important in the choice of quaternary ammonium salts. These may include interaction of the salt with the ionic components in the electrolyte,

and the influence of the salt on the viscosity, freezing point, and electrolyte wetting on the separator surface.

The effect of the bromine distribution coefficient of the quaternary ammonium salts on the cell self-discharge has been explored. The results are given in Table 5 and Figs. 7 to 9. Several important points emerge from these data.

(i) As expected, the quaternary ammonium salts with larger bromine distribution coefficients maintain lower concentrations of bromine and tribromide ions in the aqueous phase of the electrolyte. The results in Fig. 7 show that the variation in concentration of these species in the aqueous phase is dependent on the total amount of bromine left in the electrolyte. Therefore, in Fig. 9, it appears that the difference in the cell faradaic efficiency diminishes with the consumption of bromine during the cell discharge. The advantage of using quaternary ammonium salts with large bromine distribution coefficients is especially prominent with cells with a high energy capacity, due to the large amount of bromine stored initially in the electrolyte.

(ii) It can be seen from Table 5 that the cell using a quaternary ammonium salt with a large bromine distribution coefficient has a higher cell faradaic efficiency.

TABLE 5

Average cell faradaic efficiency and initial mole fraction of Br_2 in the oil phase in the electrolyte storage tank for three selected cases with different bromine distribution coefficients

	Case no.		
	1	5	6
ϵ_i^{av} (%)	82.76	87.79	90.55
$X^0_{Br2,\,oil}$	0.909	0.948	0.952

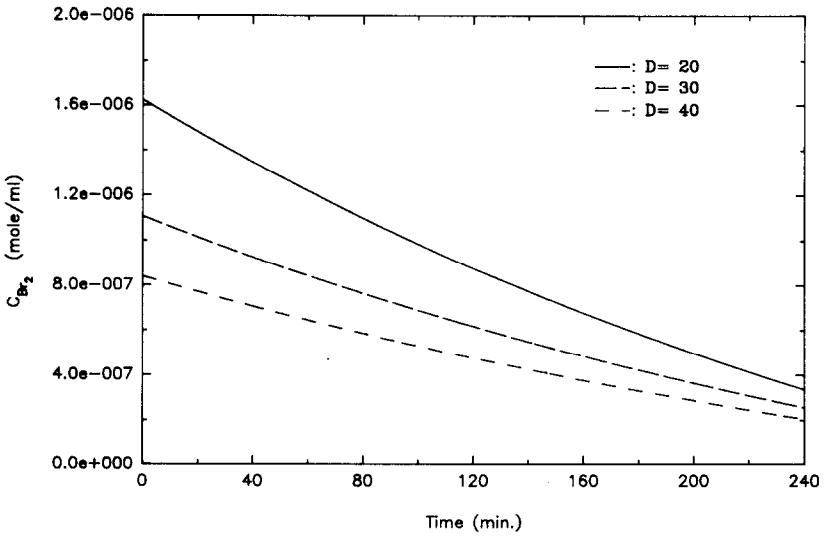

Fig. 7. Concentration of bromine in aqueous phase of the electrolyte over cell discharge period for cases with different bromine distribution coefficients.

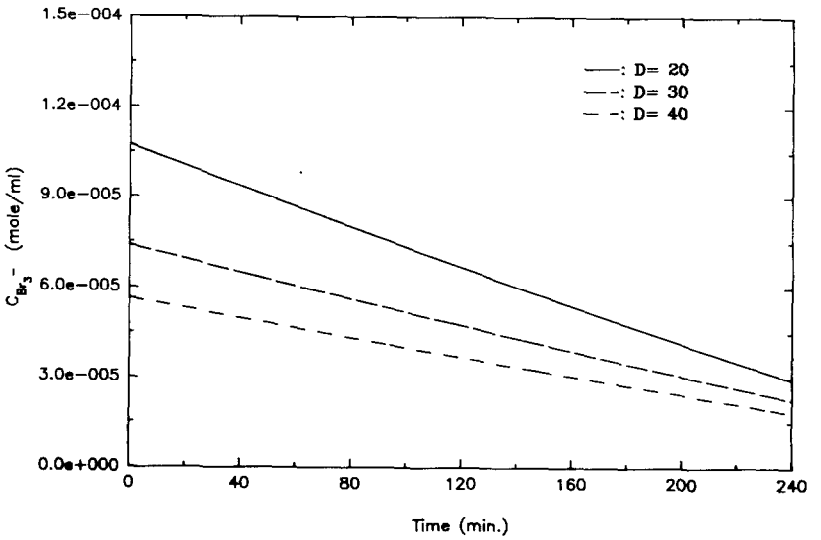

Fig. 8. Concentration of tribromide ions in aqueous phase of the electrolyte over cell discharge period for cases with different bromine distribution coefficients.

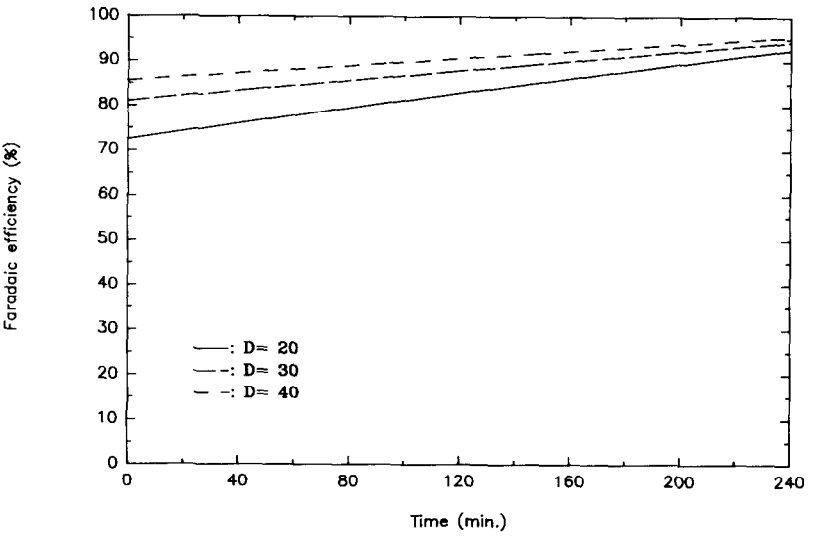

Fig. 9. Faradaic efficiency over cell discharge period for cases with different bromine distribution coefficients.

Nevertheless, the improvement gradually becomes less significant as the distribution coefficient is increased.

(iii) For Zn/Br_2 cells, the use of quaternary ammonium salts overcomes the technical problem of low energy density, which is imposed by the constraint that low concentrations of both bromine and tribromide ions must be maintained in the electrolyte to restrict the cell self-discharge rate. The results in Table 5 indicate that a quaternary ammonium

salt with a larger bromine distribution coefficient can accommodate a larger portion of total bromine in the oil phase in the electrolyte. In other words, a greater amount of bromine will be accommodated but this will not promote an increase in the cell self-discharge rate. Therefore, by virtue of the ensuring improvement in the cell faradaic efficiency and energy density, the use of quaternary ammonium salts with large bromine distribution coefficients is very beneficial to the cell performance.

Equivalent thickness of microporous plastic separators

The discussion here is confined to the use of ordinary plastic microporous separators, such as the Daramic separators manufactured by W.R. Grace. Ion-exchange membranes are excluded. The separator equivalent thickness will affect the permeability coefficient of the separator. The latter determined not only by the physical thickness and porosity/tortuosity factor of the separator itself, but also by the pretreatment of the separator. The experimental approach to determining the equivalent thickness of the separator has been discussed by Cathro *et al.* [5].

The results in Table 6 indicate that the equivalent thickness of the separator affects significantly the cell faradaic efficiency. The average cell faradaic efficiencies are 90.55, 90.55 and 93.57% for cases 4, 6 and 9, respectively (see Tables 4 to 6). These data apparently show that increasing the equivalent thickness of the separator is a very efficient way to enhance the cell faradaic efficiency. The advantages of adopting this approach include: (i) there is no increase in the electrolyte weight in the cell and (ii) it is not necessary for the cell to use a quaternary ammonium salt with a larger bromine distribution coefficient; often it is not easy to find such a salt.

A thicker separator is a very good approach to inhibiting the transport of bromine and tribromide ions through the separator; but the thickness cannot be increased unilaterally. These must be a compromise with the ohmic voltage drop due to the presence of the separator, because this ohmic resistance increases with the separator thickness. Basically, the most suitable separator thickness is a trade-off between the cell self-discharge and ohmic resistance in the separator. This can be determined by analysing the cell energy loss caused by these two phenomena.

Hydrodynamic flow condition in the electrolyte chambers

The hydrodynamic flow condition in the catholyte and anolyte chambers can affect several aspects of the cell performance, namely: (i) the pumping power consumption; (ii) the resistance for mass transport of the species in the electrolyte chambers to the separator surface, and (iii) the concentration overpotential from the electrode reactions. An increase in the flow velocity in the electrolyte chamber is necessary for cells that use electrolyte containing a low reactant concentration and designed to operate at a

TABLE 6

Average cell faradaic efficiency and voltage drop from the separator for four selected cases with different separator equivalent thicknesses

	Case no.			
	1	7	8	9
ϵ_i^{av} (%)	82.76	80.59	86.64	93.57
ΔV_S (mV)	2.75	2.2	4.18	11

TABLE 7

Average cell faradaic efficiency for four selected cases with different electrolyte volume flow velocities

	Case no.			
	1	10	9	11
ϵ_f^{av} (%)	82.76	79.86	93.57	93.20

negligible concentration overpotential from the electrode reactions. This increase, however, will also enhance the transport of the species in the electrolyte chambers to the separator surface, as well as the pumping power consumption. Therefore, the choice of a suitable hydrodynamic flow condition in the electrolyte chambers must consider these aspects.

Table 7 presents data for the average cell faradaic efficiency at different values of the electrolyte volume flow velocity in the electrolyte chambers. The electrolyte volume flow velocities of the catholyte and anolyte chambers in cases 10 and 11 are five times those in cases 1 and 9. The difference between cases 10 and 11 is the separator equivalent thickness. The results indicate that an increase of the electrolyte volume flow velocity will be harmful to the cell faradaic efficiency, but the extent of its influence depends strongly on the separator equivalent thickness. For a separator with a large equivalent thickness, an increase in the electrolyte volume flow velocity has less influence on the cell faradaic efficiency. This behaviour is due to the fact that the region where the main mass-transfer resistance is located is gradually shifted to the separator itself, as the separator equivalent thickness is increased. Therefore, the influence of the electrolyte volume flow velocity in the electrolyte chambers on the transport of the bromine and the tribromide ions through the separator becomes diminished under this condition.

The two-phase flow of the electrolyte in the bromine electrode significantly enhances the transport of bromine in the catholyte chamber region. Meanwhile, most of the bromine in the aqueous phase of the electrolyte is in the form of tribromide ions. Therefore, it can be concluded that the use of a two-phase flow in the bromine electrode will not be harmful to the cell in terms of raising the cell self-discharge rate, as a separator with a larger equivalent thickness is used in the cell.

Conclusions

An approximate mathematical model was developed for studying and estimating the cell faradaic efficiency loss caused by self-discharge in Zn/Br_2 batteries. Following conclusions can be obtained from the results of the parametric studies performed in this work.

1. Increasing the separator equivalent thickness is a very efficient way to reduce the cell self-discharge rate. The approach does not cause any increase in the electrolyte weight, nor does it demand the use of a quaternary ammonium salt with a large bromine distribution coefficient. The thickness cannot be increased unilaterally, however, and the concomitant increase in cell voltage loss due to this action must be considered.

2. The use of the quaternary ammonium salts with large bromine distribution coefficients is especially important for cells that are designed to operate with high energy capacity and high energy density. Without using these salts, the cells will suffer a higher cell self-discharge rate, and lower energy density due to the larger volume of water and quaternary ammonium salts used for preparing the electrolyte.

3. Increase in the flow velocity in the electrolyte chambers causes less of an increase in the cell self-discharge rate as the separator becomes thicker. For cells using separators with large equivalent thicknesses, the hydrodynamic flow condition in the electrolyte chambers is decided mainly by its effect on the concentration overpotential of the electrode reactions and the power loss due to electrolyte pumping, rather than by its effect on the cell self-discharge.

4. Although using two-phase flow in the bromine electrode can enhance the transport of bromine in its electrolyte chamber, the cell self-discharge rate remains unaltered because a microporous separator with a large equivalent thickness is used in the cell.

Acknowledgement

The author thanks the Energy Commission of Taiwan for financial support of this work.

List of symbols

A	electrode area, cm^2
b	electrolyte chamber thickness, cm
$C_{i,A}$	concentration of species i in the anolyte chamber, mol cm^{-3}
C_i^{av}	average concentration of species i in the catholyte chamber, mol cm^{-3}
C_i	inlet concentration of species i to the catholyte chamber, mol cm^{-3}
$C_{Br_2,oil}$	inlet concentration of Br_2 in the oil phase to the catholyte chamber, mol cm^{-3}
C_i^{out}	outlet concentration of species i from the catholyte chamber, mol cm^{-3}
$C_{Br_2,oil}^{out}$	outlet concentration of Br_2 in the oil phase from the catholyte chamber, mol cm^{-3}
C_i^0	initial inlet concentration of species i to the catholyte chamber, mol cm^{-3}
$C_{Br_2,oil}^0$	initial inlet concentration of Br_2 in the oil phase to the catholyte chamber, mol cm^{-3}
D	distribution coefficient
D_i	diffusivity of species i, $cm^2\ s^{-1}$
d_S	separator equivalent thickness, cm
d_h	hydraulic diameter, cm
F_{aq}	volume flow velocity of the aqueous phase into the catholyte chamber, ml sec^{-1}
F_{oil}	volume flow velocity of the oil phase into the catholyte chamber, ml sec^{-1}
F_{Zn}	volume flow velocity into the anolyte chamber, $cm^3\ s^{-1}$
f	Faraday's constant
h	electrolyte chamber width, cm
i	current density, A cm^{-2}
K_{eq}	equilibrium constant for tribromide reaction, M^-

$K_{i,C}$	mass-transfer coefficient of species i on the cathode side of the separator, cm s^{-1}
$K_{i,A}$	mass-transfer coefficient of species i on the anode side of the separator, cm s^{-1}
$K_{i,ov}$	overall mass-transfer coefficient of species i, cm s^{-1}
l	electrode length, cm
N_i	mass flux of species i through separators, mol cm^{-2} s^{-1}
n^0_{Br2}	total moles of Br_2 initially added to the electrolyte storage tank, mol
$n^0_{Br^-}$	total moles of Br^- initially added to the electrolyte storage tank, mol
P_S	permeability coefficient of the separator, cm s^{-1}
Re	Reynolds number
Sc	Schmidt number
Sh_{av}	average Sherwood number
T	cell operating time, s
t	time, s
t_{Br^-}	transference number of Br^-
V_{oil}	volume of the oil phase in the electrolyte storage tank, cm^3
V_{aq}	volume of the aqueous phase in the electrolyte storage tank, cm^3
v	linear flow velocity, cm s^{-1}
$X_{Br2,oil}$	mole fraction of Br_2 in the oil phase in the electrolyte storage tank

Greek letters

ϵ_i	faradaic efficiency
ϵ_i^{av}	average faradaic efficiency
ν	kinematic viscosity, cm^2 s^{-1}
κ_S	electrolyte conductivity, Ω^{-1} cm^{-1}
ΔV_S	voltage drop across the separator, V

References

1 T. Fujii and M. Kanazashi, *Prog. Batteries Solar Cells, 5* (1984) 31.
2 J.J. Bolstad and R.C. Miles, *Proc. 24th Intersociety Energy Conf., 899089, Aug. 6–11, 1989, Washington, DC, USA.*
3 T. Hashimoto, H. Itoh and A. Hirota, *Proc. 3rd Int. Conf. Batteries for Utility Energy Storage, Kobe, Japan, Mar. 18–22, 1991.*
4 F.G. Will, in J. Thompson (ed.), *Power Sources 7,* Academic Press, London, 1979, p. 313.
5 K.J. Cathro, K. Cedzynska and D.C. Constable, *J. Power Sources, 16* (1985) 53.
6 M.J. Mader and R.E. White, *J. Electrochem. Soc., 133* (1986) 1297.
7 D.J. Eustace, *J. Electrochem. Soc., 127* (1980) 528.
8 E. Klein, R.A. Ward and R.E. Lacey, Membrane processes — dialysis and electrodialysis, in R.W. Rousseau (ed.), *Handbook of Separation Process Technology,* Wiley, New York, 1987.
9 K.J. Cathro, D.C. Constable and P.M. Hoobin, *J. Power Sources, 22* (1988) 29.
10 I. Roušar, J. Hostomký, V. Cezner and B. Šterak, *J. Electrochem. Soc., 118* (1971) 881.
11 P.-Y. Lu and R.C. Alkire, *J. Electrochem. Soc., 131* (1984) 1059.